International Journal of the Korean Society of Precision Engineering, Vol. 1, No. 1, June 2000.

Measurement Resolution of Edge Position in Digital Optical Imaging

Sang-Yoon Lee* and Seung-Woo Kim**

*Intek Engineering Co. Ltd., Taejon, South Korea
**Dept. of Mechanical Engineering, Korea Advanced Institute of Science and Technology, Taejon, South Korea

ABSTRACT

The semiconductor industry relies on digital optical imaging for the overlay metrology of integrated circuit patterns. One critical performance demand in the particular application of digital imaging is placed on the edge resolution that is defined as the smallest detectable displacement of an edge from its image acquired in digital from. As the critical feature size of integrated circuit patterns reaches below 0.35 micrometers, the edge resolution is required to be less than 0.01 micrometers. This requirement is so stringent that fundamental behaviors of digital optical imaging need to be explored especially for the precision coordinate metrology. Our investigation reveals that the edge resolution shows quasi-random characteristics, not being simply deduced from relevant opto-electronic system parameters. Hence, a stochastic upper bound analysis is made to come up with the worst edge resolution that can statistically well predict actual indeterminate edge resolutions obtained with high magnification microscope objectives.

Key Words : Digital optical imaging, edge resolution, worst upper bound edge resolution, overlaymetrology, microscope objectives.

1. Introduction

In manufacture of integrated circuit patterns, digital optical imaging is currently being used as a key technology for the overlay metrology to assess the layer-to-layer registration capabilities of lithography equipment. The overlay metrology is carried out by quantifying the relative registration of two box-shaped marks, one patterned in photoresist and the other in a previous layer. The center coordinates of each box are located from the measured intensity profiles of its line edges on the assumption of symmetry as illustrated in Figure 1. One critical performance index in this metrology turns out to be the edge resolution, which represents the measurement sensitivity of digital optical imaging being exerted on monitoring line patterns edges. The challenge for the optical overlay metrology comes from semiconductor process technologies that are being pursued on a timetable consistent with the SIA Roadmap1 shown in Table 1.

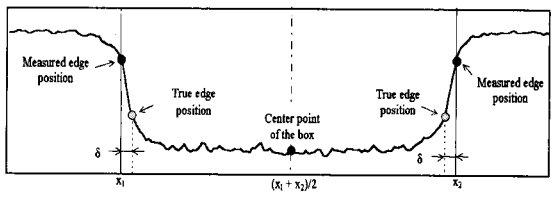

Fig. 1 Use of symmetry on locating center point

Table 1 Timetable for overlay metrology

DRAM production	1995	1998	2001	2004	2007	2010
Feature size (nm)	350	250	180	130	100	70
Overlay tolerance (nm)	100	75	50	40	30	20
OL Metrology tool budget (nm)*	10	8	5	4	3	2

* Assumes advanced techniques to maximize usable depth-of-focus

As the circuit feature size reduces to 0.18 mm, the projected metrology tool budget should be in the order of 10 nm or less. This stringent requirement places new demands on the overlay measurement capabilities so that thorough understanding on the ultimate resolution limit of optical digital imaging in edge location becomes necessary.

Digital optical imaging for the overlay metrology is performed using four basic components illustrated in Figure 2; the illumination optics with a light source, the imaging objective, the electronic image acquiring device, and a digital computer for image data processing.

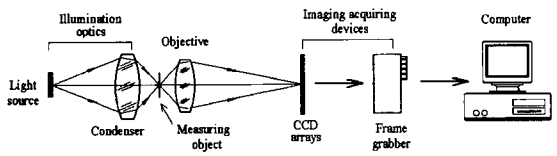

Fig. 2 Basic configuration of digital imaging system

In this digital imaging system, the edge resolution is defined as the smallest variation of the edge position that is detectable from the output signal finally obtained in digital form. The edge resolution becomes meaningful not only in describing the output signal sensitivity but also in predicting the ultimate measurement uncertainty of digital optical imaging in locating pattern edges. One intuitive form of expressing the edge resolution is the so called effective pixel resolution, which is simply obtained by dividing the actual one pixel size by the magnification of the objective. This term in fact represents the effective pixel size being reflected on the object plane, but it hardly provides a precise estimation for the measurement resolution since it excludes the image resolving characteristics of the objective and the quantization effects of the image acquiring electronics. Consequently, experience proves that the effective pixel resolution usually provides an inaccurate underestimation that usually turns out to be far worse than actual resolutions practically achieved.

2. Measurement resolution

Figure 3 schematically illustrates the processing sequences through which the digital image of a line edge is acquired.

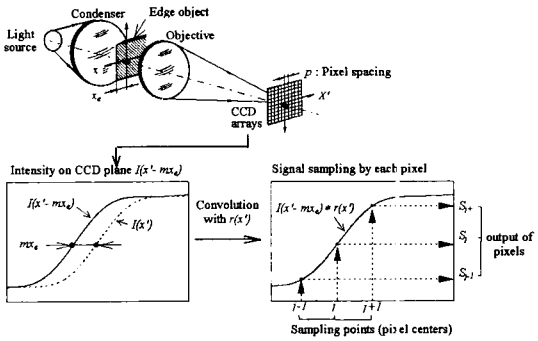

Fig. 3 Digital image sampling process

A representative single line edge is located at the position of x= x_e on the object plane. The illumination is assumed to be perfectly incoherent for convenience of analysis. Then, the image intensity distribution of the line edge is obtained in the normalized form of

$$I(x' - m\,x_e) = \frac{1}{2} + \frac{1}{\pi} Si[\frac{4\pi N_o}{\lambda m}(x' - m\,x_e)] - \frac{1}{\pi}\cos[\frac{4\pi N_o}{\lambda m}(x' - m\,x_e)]/[\frac{4\pi N_o}{\lambda m}(x' - m\,x_e)] \quad (1)$$

in which x' denotes the image coordinate; No and m the numerical aperture and magnification of the objective, respectively; λ the mean wavelength of illumination light; and Si[ξ] the sine integral of ξ .

Being affected by light diffraction, the intensity distribution of Eq.(1) becomes a smoothed profile spanning multiple pixels as graphically shown in Figure 4.

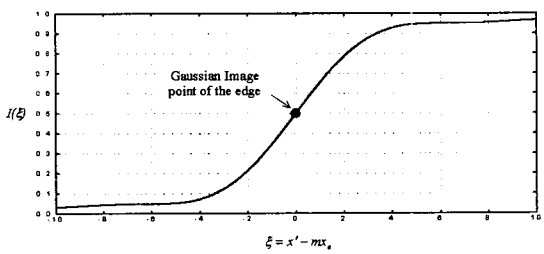

Fig. 4 Normalized intensity profile of the edge under incoherent illumination

The Gaussian image point of the line edge is found at x' = mxe , where its corresponding normalized intensity level becomes always 0.5. A CCD array discretely samples the intensity profile, whose analog output from each pixel is described as

$$S_j(x_e) = \int_{-\infty}^{+\infty} I(x' - m x_e) r(jp - x') dx'. \quad (2)$$

In the above, the subscript j represents the pixel index; p the pixel pitch; and r(ξ) the point spread function of the pixels that may be approximated as the rectangular function of

$$r(\xi) = \frac{1}{p} Rect[\frac{\xi}{p}]. \quad (3)$$

The sampled signal is then quantized by an analog-to-digital converter, whose output becomes a gray level integer of

$$G_j(x_e) = int[k\, S_j(x_e)]. \quad (4)$$

The function int[ξ] truncates the decimal fraction of ξ . Thus the output Gj(xe) becomes an integer ranging from 0 to k. .

Now, the edge resolution is defined as the smallest variation of edge position that is detectable from the output signal obtained in digital form. More specifically, it means the minimum displacement of the edge position that causes the change of unit gray level in any of Gj(xe) for j = ..., -1, 0, 1, ... To derive the edge resolution in an explicit form, two variables δ_j^p and δ_j^n are defined for each pixel such that δ_j^p represents the displacement of the edge position to be induced in the positive x-direction to bring about unit change in Gj(xe), while δ_j^n the displacement in the negative x-direction for the same purpose. As depicted in Figure 5, the two variables are obtained as

$$\delta_j^p = \frac{D_j(x_e)}{k S'_j(x_e)} \text{ and } \delta_j^n = \frac{1 - D_j(x_e)}{k S'_j(x_e)}, \quad (5)$$

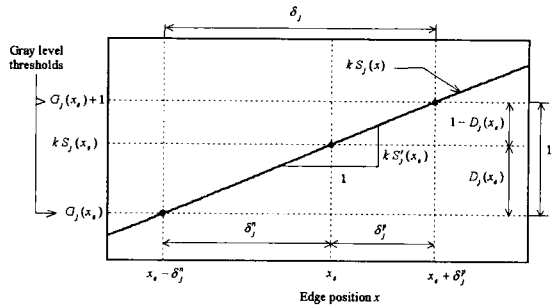

Fig. 5 Derivation of δ_j^p, δ_j^n, and δ_j

where Dj(xe) represents the truncated fraction of kSj(xe) during the quantization process, i.e.,

$$Dj(xe) = kSj(xe) - Gj(xe). \quad (6)$$

In Eq.(5), Sj'(xe) denotes the partial derivative of Sj(xe) with respect to xe. This can be derived from Eq.(2) such as

$$Sj'(xe) = \frac{\partial S_j(x_e)}{\partial x_e}.$$

$$= \frac{m}{p}[I(m x_e - jp + \frac{p}{2}) - I(m x_e - jp - \frac{p}{2})] \quad (7)$$

Each pixel has different values of δ_j^p and δ_j^n, depending on its own Dj(xe) and Sj(xe). Among all δ_j^p, let be $\delta_{\min}^p$ the smallest, i.e.

$$\delta_{\min}^p = Min[\delta_j^p] = Min[\frac{D_j(x_e)}{k S_j'(x_e)}]. \quad (8)$$

Then $\delta_{\min}^p$ becomes the minimum displacement of the edge position to be induced in the positive x-direction to produce one gray level change in a most sensitive pixel. Similarly, another displacement $\delta_{\min}^n$ is defined in negative x-direction such as

$$\delta_{\min}^n = Min[\delta_j^n] = Min[\frac{1 - D_j(x_e)}{k S_j'(x_e)}] \quad (9)$$

Consequently, as long as the edge position stays within the range of xe - δ^{n}_{min} < x < xe + δ^{p}_{min}, the whole digital image data remain unchanged. Hence, the edge resolution can be deduced as

$$R(xe) = \delta^{n}_{min} + \delta^{p}_{min} = Min[\frac{D_j(x_e)}{k S_j'(x_e)}] + Min[\frac{1 - D_j(x_e)}{k S_j'(x_e)}]. \quad (10)$$

Now it is noted that the edge resolution R(xe) does not come out as a constant but varies with the edge position xe. in addition, its variation with xe becomes highly nonlinear due to the operation of Min[·] performed on multiple pixel data. Figure 6 shows a typical example computed for a specific opto-electronic configuration, in which the edge resolution was plotted against xe over one effective pixel pitch interval of p/m. The computed edge resolution repeats its pattern with a period of p/m as xe further increases or decreases. It is clearly seen that the result tends to oscillate too severely to be represented by a constant, exhibiting a quasi-stochastic behavior as being presented by the scattered dots in the figure. It would therefore be more meaningful to describe the edge resolution in statistical terms of its mean along with standard deviation.

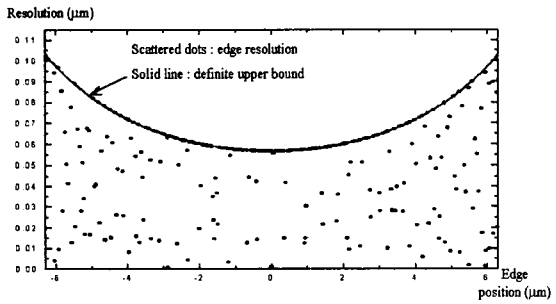

Fig. 6 Edge resolution and its definite upper bound over one pixel range

3. Stochastic approach

The first step to treat the edge resolution in statistical way is to find its appropriate probability distribution function. For this, let us consider the interval $\delta_j = \delta^{p}_{j} + \delta^{n}_{j}$, of the j-th pixel as indicated in Figure 5. In fact, the interval δ_j represents the individual edge resolution when only the j-th pixel is considered for locating the edge. In other words, during the interval δ_j, the occurrence probability of the event that Gj(xe) would change its value is unity. From Eq.(5), the interval δ_j is obtained as

$$\delta_j = \frac{1}{k S'_j(x_e)}. \quad (11)$$

Now that the gray level change of Gj(xe) happens once per interval, δ_j the expected frequency of this event over unit interval becomes

$$f_j = \frac{1}{\delta_j} = k S'_j(x_e) \quad (12)$$

This consideration is extended to include all the pixels concerned, so that the total expected frequency of this event over unit interval becomes the summation of f_j , i.e.

$$f = \sum_j f_j = k \sum_j S'_j(x_e). \quad (13)$$

Or, by substituting Eq.(7) into Eq.(13), the total expected frequency is determined as

$$f = k \sum_j S'_j(x_e) = \frac{mk}{p}[I(\infty) - I(-\infty)] = \frac{mk}{p}[1 - 0] = \frac{mk}{p} \quad (14)$$

If it is assumed that occurrence of each event is independent of one another, then the probability function of R(xe) may be assumed to be an exponential distribution of

$$Pr[R(x_e) < r] = 1 - \exp(-\frac{mk}{p} r). \quad (15)$$

Accordingly, the mean resolution Rm and standard deviation σ are determined, respectively, such as

$$R^m = \int_0^\infty \frac{d\Pr}{dr} r dr$$

and

$$\sigma^2 = \int_0^\infty \frac{d\Pr}{dr} (r - R^m)^2 dr \quad (16)$$

It is noted that the exponential distribution produces the standard deviation identical to the mean. From these two statistical terms, the upper bound of the edge resolution is taken as the value of (Rm +5 σ) which guarantees 99.8 per cent reliability, i.e.,

$$R(x_e) \le \frac{6p}{mk} \equiv R_s^u. \quad (17)$$

Hereafter, R_s^u is referred to as the probabilistic upper bound of the edge resolution. From practical point of view, the upper bound is meaningful as it statistically describes the worst limit of the edge resolution. It is worth noting that the probabilistic upper bound is decided only by three system parameters; p the pixel pitch, m the magnification, and k the number of quantization level. Other parameters such as the numerical aperture No or the light wavelength λ have no effects on the probabilistic upper bound.

In addition to the probabilistic upper bound, another upper bound may also be considered which in fact can be derived in a deterministic way. The expression of Eq.(10) may be extended to an inequality condition of

$$R(x_e) = Min[\frac{D_j(x_e)}{k S_j'(x_e)}] + Min[\frac{1 - D_j(x_e)}{k S_j'(x_e)}]$$

$$\le Min[\frac{D_j(x_e) + 1 - D_j(x_e)}{k S_j'(x_e)}]$$

$$\le Min[\frac{1}{k S_j'(x_e)}] \quad (18)$$

This means that the edge resolution R(xe) considering all the pixels becomes always smaller than any individual edge resolution of a single pixel. Hence, the upper bound of R(xe) may be regarded as the minimum among all the individual edge resolutions, which can be written as

$$R_D^u = \frac{1}{k\, Max[S_j'(x_e)]}. \quad (19)$$

When the illumination is incoherent, the maximum of Sj'(xe) always occurs at the Gaussian image point of the line edge, i.e. x' = mxe, which corresponds to the point ξ =0 in the image profile given in Figure 4. Therefore, using Eq.(7), R_D^u is explicitly obtained as

$$R_D^u = \frac{p}{mk[I(m x_e + \frac{p}{2}) - I(m x_e - \frac{p}{2})]}. \quad (20)$$

Back in Figure 6, R_D^u is presented in the solid line. It is seen that R_D^u also varies with xe like R(xe) and reaches its maximum when xe = ±(p/m). The maximum, denoted by R_D^U is given as

$$R_D^U = \frac{p}{mk[I(p) - I(0)]} \quad (21)$$

Now R_D^U is defined as the definite upper bound of the edge resolution, in contrast with R_s^u previously defined as the probabilistic upper bound. By substituting Eq.(1) into Eq.(21), R_D^U is obtained in a deterministic form of

$$R_D^U = C\frac{p}{mk},$$

where

$$C = \pi \{Si[\frac{4\pi N_o}{\lambda m} p] - \cos(\frac{4\pi N_o}{\lambda m} p)/(\frac{4\pi N_o}{\lambda m} p)\}^{-1}. \quad (22)$$

4. Worst edge resolution

So far, two upper bound limits of edge resolution have been derived; the probabilistic R_S^U of Eq.(17) and deterministic R_D^U of Eq.(22). Now it becomes necessary to define the worst edge resolution that can predict actual edge resolutions more reliably.

if $R_D^U < R_S^U$, it is rational to take the definite upper bound R_D^U as the worst. On the contrary, in case $R_S^U < R_D^U$, the probabilistic upper bound R_S^U

would be more appropriate. Consequently, the worst resolution, denoted by RW, is decided as

$$R^W = Min(R_D^U, R_S^U). \tag{23}$$

The critical condition under which R_D^U becomes equal to R_S^U is found by equating Eq.(17) to Eq.(22) such as

$$\pi\{Si[\frac{4\pi N_o}{\lambda m} p] - \cos(\frac{4\pi N_o}{\lambda m} p)/(-\frac{4\pi N_o}{\lambda m} p)\}^{-1} = 6. \tag{24}$$

This can be readily solved by numerical computation to give out the condition of

$$\frac{N_o p}{\lambda m} = 0.085. \tag{25}$$

This means that if Nop/(λ m) is larger than 0.085 , the definite upper bound R_D^U is taken as RWand vice versa. In most configurations of digital imaging using commercially available microscope objectives, the value of Nop/(λ m) turns out to be larger than 0.085. Therefore the worst edge resolution can be safely given by

$$R^W = R_D^U = C\frac{p}{mk}. \tag{26}$$

Table 2 shows some exemplary worst edge resolutions that were computed using Eq.(26) with six different objectives.

Table 2 Some typical values of worst edge reolution

Probe #	#1	#2	#3	#4	#5	#6
NA	0.025	0.055	0.14	0.42	0.55	0.7
magnification	1	2	5	20	50	100
worst edge res.(μm)*	0.109	0.0542	0.022	0.0055	0.00253	0.00172

*All the above resolutions were computed with respect to a CCD camera of 12.6μm spacing, with λ=550 nm

It is worth noting that the worst resolution becomes less than 0.01 micrometer for the objective of 20X magnification with 0.42 NA, and further it reaches 1.7 nm for the objective of 100X magnification with 0.7 NA. Now, to verify this theoretical result, experiments were also performed using the apparatus setup shown in Figure 7.

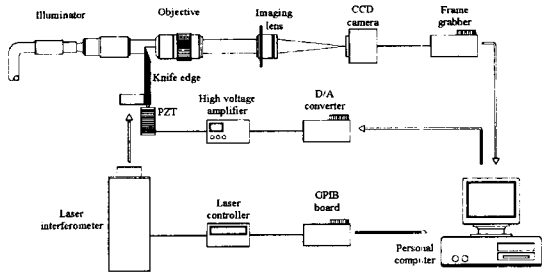

Fig. 7 Experimental setup for resolution measurement

A knife edge was used as a measuring object, whose lateral movement is precisely controlled using a piezoelectric actuator and a heterodyne laser interferometer with a nanometer resolution. Figure 8 shows a typical intensity profile of the knife edge that was monitored from a single pixel of the CCD camera while moving the knife edge by approximately 0.05 micrometer step. The measured data were compared with the theoretical variation of the gray level computed using Eq.(4).

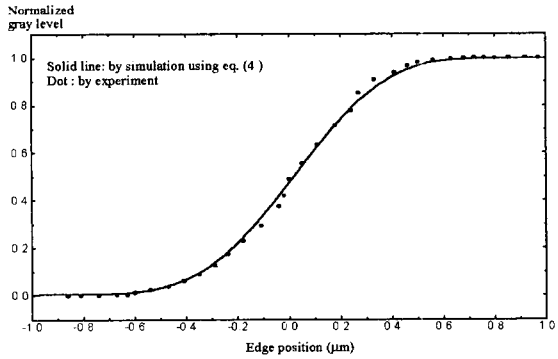

Fig. 8 Output variations of a pixel with respect to edge point movement

It is seen that the measured data are well predicted by the theoretical estimation, which is presented by the solid line in the figure. Now, actual edge resolutions were measured for six different objectives installed in the same experimental setup of Figure 7. Table 3 summarizes the comparisons made between the theoretical and experimental results, which are in good agreements with about 10 %

discrepancy.

Table 3 Experimental result of worst edge resolution

Probe #	#1	#2	#3	#4
NA	0.025	0.055	0.14	0.42
R_D^U theoretical (μm)	0.109	0.0542	0.022	0.0055
R_D^U experimental (μm)	0.126	0.056	0.027	0.006
% of error	13%	3%	18%	8%

5. Conclusions

The edge resolution of digital optical imaging has been defined as the minimum displacement of the edge position that is detectable from the acquired digital image of the line edge. This term is found useful in predicting the actual measurement sensitivity and uncertainty of digital optical imaging especially in the overlay control of integrated circuit patterns. The edge resolution is deterministic, but it shows a quasi-random behavior that can not be simply described in terms of relevant opto-electronic system parameters. Hence a stochastic approach has been made to describe the indeterminate edge resolution in term of the worst upper bound. Computer simulation and experimental results proves that the worse edge resolution can be usefully used in predicting actual resolutions obtained with microscope objectives.

Reference

1. M. Levenson, "Extending optical lithography to the gigabit era," Microlithography World, Autumn, pp. 5, 1994.
2. M. Takashima, K. Baba, S.Yamamura, A. Ushirogawa and T. Shiga, Precision pitch measuring system for optical fiber array at multiplier-fiber connector end, Annals of the CIRP, Vol. 29, No. 1, pp. 377-380, 1980.
3. P. Morantz, A nanometric precision non-contact toolsetting system, Proc. of 7th Annual Meeting ASPE, pp. 18-21, 1992.
4. K. Maruyama, H. Tsuji, and K. Hashimoto, Development of subpixel edge probe with high resolution and application for Coordinate Measuring Machine, Proc. of 9th Annual Meeting ASPE, pp. 129-132, 1994.
5. E. Doebelin, Measurement Systems Application and Design, pp. 73, McGraw-Hill, 4th ed.
6. C.-S. Ho, Precision of digital vision systems, IEEE Trans. Pattern Anal. Machine Intell, Vol. PAMI-5, No. 6, pp. 593-601, 1983.
7. H. Tonshoff, H. Janocha and M. Seidel, Image processing in a production environment , Annals of the CIRP, Vol.37, No.2, pp. 579-590, 1988.
8. M. Tichem and M. Cohen, Submm registration of fiducial marks using machine vision , IEEE Trans. Pattern Anal. Machine Intell, Vol. 16, No. 8, pp. 791-794, 1994.
9. J. Schaefer, S. Kaiser and T. Carrington, The development of a non-contact diamond tool alignment and measuring system, Proc. of 9th Annual Meeting ASPE, pp. 358-361, 1994.
10. Q. Tian and M. Huhns, Algorithms for subpixel registration, Computer Vision, Graphics, and Image Processing, Vol. 35, pp. 220-230, 1986.
11. P. Considine, Effect of coherence on imaging systems, J. Opt. Soc. Am., Vol. 56, No. 8, pp. 1001- 1009, 1966.
12. M. Marchywka and D. Socker, Modulation transfer function measurement technique for small-pixel detectors, Applied Optics, Vol. 31, No. 34, pp. 7198-7213, 1992.
13. K. Winick, Cramer-Rao lower bounds on the performance of charge-coupled-device ptical position estimators, J. Opt. Soc. Am. A, Vol. 3, No. 11, pp. 1809- 1815, 1986.